Exploiting 3D Printed Substrate
for Microfluidic SIW Sensor

Stefano Moscato, Marco Pasian, Maurizio Bozzi, Luca Perregrini
Department of Electrical, Computer and Biomedical
Engineering, University of Pavia
Pavia, Italy
stefano.moscato01@universitadipavia.it

Ryan Bahr, Taoran Le, Manos M. Tentzeris
The School of Electrical and Computer Engineering
Georgia Institute of Technology
Atlanta, U.S.A.
rbahr@gatech.edu

Abstract—**This paper exploits the possibility of the 3D printing for microwave sensor purposes. Because of the complex shapes allowed by this emerging technology, a fully-custom microfluidic sensor can be embedded directly during the substrate preparation. By this way, a simple approach in sensor design can be achieved together with a reduction of the manufacturing time, costs and overall complexity of the sensor. 3D printed microwave devices are very attractive for the future generation of Wireless Sensor Networks and of the Internet of Things. The proposed microfluidic sensor exploits the substrate integrated waveguide technology to keep high the quality factor and to merge the requirements of planar integration of further blocks. The aim of this sensor is a real time characterization of fluids across the lower UWB frequency band. The design, a first prototype and measurements are shown to exhibit the potentiality of this technique.**

Keywords—**Substrate integrated waveguide (SIW), wireless sensor networks (WSN), Internet of Things (IoT), Microfluidic, 3D printing technolgies.**

I. INTRODUCTION

The 3D printing manufacturing technique is becoming one of the most important topic in the science and engineering panorama. Because the cost of this emerging technology is lowering in the last few years, nowadays this manufacturing process is widely adopted by industries and companies in various fields, electronics in example [1].

The most important feature of a 3D printer is the possibility to realize very complex shapes and geometries. This characteristic can be achieved because the process is additive: each layer of material is dropped off by the 3D printer and empty volumes can be manufactured in solid objects. These possibilities are clearly more difficult for subtractive process, milling in example, that can realize shapes only by removing external material.

In addition, 3D printers can lay down different materials, both dielectric and metallic. Different materials are also related to different technique of deposition, for example bulky metals can only be printed with very expensive printers called laser sintering printers [2]. The most adopted 3D printers exploit the fused deposition modeling (FDM) that permits to drop off layers of plastic material. Among the most common and commercialized materials take place the acrylonitrile butadiene styrene (ABS), the polylactic acid (PLA) and flexible or eco-friendly materials.

This technology is very promising for fully-custom designs of microwave components. Firstly because together with the spreading of this technology also the performance (in terms of printing precision and accuracy) are growing, and because the large availability of printers and material gives a lot of new opportunities to the designers. These kinds of features well fit to the demand of microwave components for the new generation of wireless sensor networks (WSN) [3] and to increase the possibilities given by the Internet of Things (IoT).

The 3D printing technology can be adopted for microwave microfluidic sensors thus achieving a complete Lab-on-Chip approach. No fabrication method allows pipes or cavities manufactured inside the dielectric substrate without involving a multilayer approach or silicon technologies. Microwave and microfluidic planar sensors are well known in the literature and generally involved microstrip comb fingers [4] or ring resonators [5], both on standard substrate or printed on paper material [6]. Generally, the microfluidic part is achieved by realizing a pipe on the top of the substrate so the fluid under test flows between small gaps. On one hand this approach is the simple one but in the other hand, the sensitivity with respect of different fluids tested can be poor.

The novelty introduced in this work concerns the possibility of manufacturing a multi-folded pipe directly embedded into the substrate. This approach leads to a high change of dielectric properties of the substrate when a fluid flows in the pipe with the result of a high sensitivity. Moreover, a substrate integrated waveguide (SIW) square cavity can be adopted in order to keep as high as possible the quality factor and to match the requirements of planar technology [7] for the implementation of further blocks, as schematically depicted in Fig. 1.

This paper is organized in five sections that cover the electromagnetic characterization of the adopted material

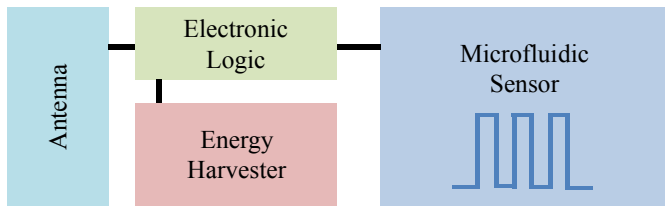(Section II), the design of the sensor (Section III) and the simulation results (Section IV).

Fig. 1 Block diagram of an autonomous and complete device capable of sensing and data transmission.

II. T-GLASE CHARACTERIZATION

The substrate characterization is mandatory when dealing with an innovative material and with a non-standard fabrication process. Nevertheless several articles report the electromagnetic properties of the 3D printed materials [8], a new one has to be carried out because the same material can exhibit different properties. These changes are related to the different settings of the 3D printer such as the extrusion speed and temperature and the infill pattern.

The chosen material is t-glase by Taulman3D [9]. This material was developed for optical applications and it is chosen because derives directly from the highest quality of PET, so lower losses with respect of other 3D printed materials are expected. The adopted printer is the Metal Plus made by Printrbot [10], a commercial available printer able to drop off extruded plastic material with very high accuracy. This machine is capable of a reliable vertical resolution of 0.1 mm and therefore it is suitable for the fabrication of small empty pipes within the dielectric substrate.

The technique adopted to characterize this material was proposed in [11] and was employed to estimate the dielectric permittivity and the loss tangent of fabric. This method combines both a simple manufacturing technique and a wideband characterization. In particular, this project is intended for the first part of the UWB frequency band (3.1-4.8 GHz) but future developments could be carried out to exploit the whole frequency band.
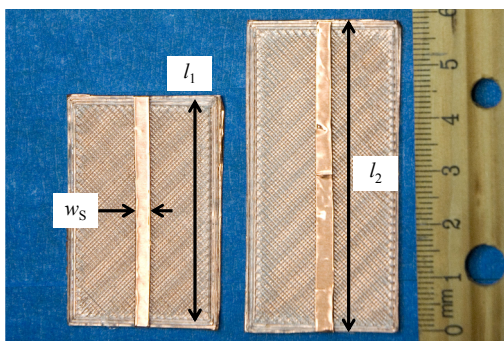

Fig. 2 The manufactured microstrip transmission lines on t-glase substrate.
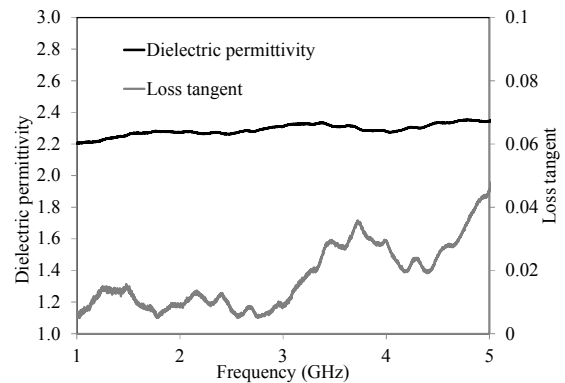

Fig. 3 Dielectric permittivity and loss tangent of the t-glase substrate.

Two microstrip transmissions lines with different lengths are designed and manufactured on a 1.20 mm thick t-glase substrate with a 100% rectilinear infill. The first one is 45 mm long (l_1) and the second one is 60 mm long (l_2), as shown in Fig. 2. Both microstrips have the same width (w_S) equal to 3 mm.

The length difference between them is up to the 25% and it is enough for a good estimation of the electromagnetic properties of the substrate. Finally, SMA-to-coaxial transitions are adopted to connect them with a vector network analyzer (VNA) in order to collect the S parameters, in magnitude and phase.

Thanks to this approach, the dielectric permittivity and the loss tangent are retrieved. The substrate exhibits an ε_r equal to 2.3 and an average tanδ of 0.02 across the frequency band of interest, as shown in Fig. 3.

III. DESIGN AND MANUFACTURING OF SIW MICROFLUIDIC SENSOR

Once the material is known, the microfluidic sensor can be designed with the aid of a full-wave commercial software. The starting point is a square SIW cavity designed on a 100% infill t-glase substrate thick enough to guarantee sufficient vertical space to the microfluidic system.

An architecture of pipes is designed directly embedded in the substrate. Several configurations of tubes have been simulated and the chosen one is a single multi-folded pipe. Two vertical exits are designed in order to guarantee a continous flow of fluid within the pipe. Both pipes and exits have the same diameter (d_P).

In order to increase the frequency shift due to the presence of fluid, the architecture of the pipese is optimized to fill as much as possibile the SIW cavity. The length of the pipes (l_P), their reciprocal spacings (s_P) and their numbers are chosen following the aforementioned principle but also by keeping in account the limits of the fabrication process. The last parameter that could be optimized is d_P. This value is bounded by the accuracy of the 3D printer and the thickness of the substrate. Because these boundaries are very close, the diameter of the pipes is practically fixed.
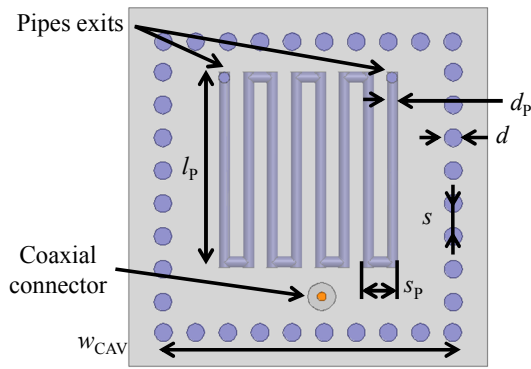
Fig. 4 The layout of the proposed sensor. The pipes are realized inside the substrate. The dimensions of this desig are w_{CAV}=42.5 mm, l_P=28.6 mm, s_P=5.1 mm, d_P=1.6 mm, d=2.59 mm, s=4.8 mm.
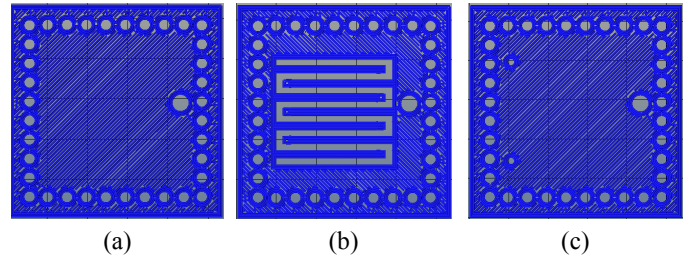

Fig. 5 This sequence explains how the slicer works: (a) is the first layer where only the hole for the SMA connector is visible, (b) it is the middle layer where the folded pipe is well defined. Finally, (c) is the last layer where also the exits are realized.

Next, the SIW cavity is designed in order to exhibit the resonance frequency of the TM_{110} fundamental mode in the lower part of the UWB frequency band. Moreover, the highest frequency shift expected is 1 GHz when distilled water (because of its high dielectric permittivity) flows into the pipe. This shift brings the resonance frequency of the cavity close to 3.1 GHz that is the starting frequency of the UWB range. This point is essential when dealing with WSN and wireless systems in general: by adopting this frequency band, a future implementation with other UWB blocks will be easier.

The SIW technology requires rows of metallized via in order to guarantee a lateral shield along the sides of the cavity. At this moment, the possibility of printing metallic vias is not available. Because of this, rivets are used guarantee the highest ohmic contact between the top and the bottom ground plane, metallized with standard adhesive aluminum tape. The dimensions of the chosen rivets affects the substrate thickness (t=4 mm) and the vias diameter (d). The pitch between the holes (s) is optimized to fit the posts in the cavity edge (w_C). The value of the pitch is upper bonded by the golden rule that set the reciprocal spacing equal to the double of the diameter in order to decrease as much as possible the radiation leakege [7].

The microwave cavity has to be excited by an external source. The chosen configuration concern a SMA panel connector that directly feeds the cavity with its pin. Because only one port is arranged, the frequency behaviour can be observed by the S_{11} parameter.

Once the design is ready to be manufactured, the model has to be virtually cutted into layers. Each layer is printed in sequence: from the bottom to the top of the structure, as shown in Fig.5. The software that controls the 3D printer estimates to employ 3788 mm of t-glase filament that is extruded at 240°C for 112 minutes.

Fig. 6 shows the first printed prototype. Four cylindrical pads are also realized at each corner. These pads are required because many 3D printed materials tend to lift from the bed where they are manufactured. The higher is the printed area at the corners, the higher are the chances to avoid this phenomenon. Fig. 6 also shows the vertical exits of the pipes and the space where the panel SMA connector has to be placed.

Because the tube is embedded into the substrate, there is no possibility to estimate the accuracy in pipes realization. One possibility is to realize one more prototype and slice it. But because of the high stiffness of t-glase, cracks within each layer or along the substrate may occur. Nevertheless, an optical inspection is carried out by carefully looking the sensor adopting a light source behind it. Fig. 7 highlights the internal architecture of pipes and it is possible to observe fabrication accuracy of each tube.
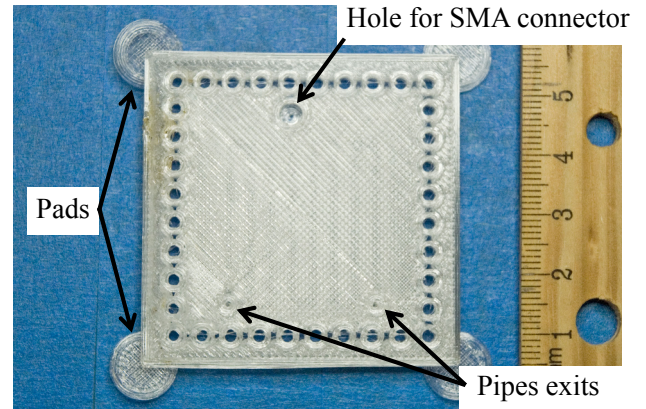

Fig. 6 Top view of the first prototype of the 3D printed microfluidic SIW sensor. Pads, the hole for the SMA connector and pipes exits are highlighted.
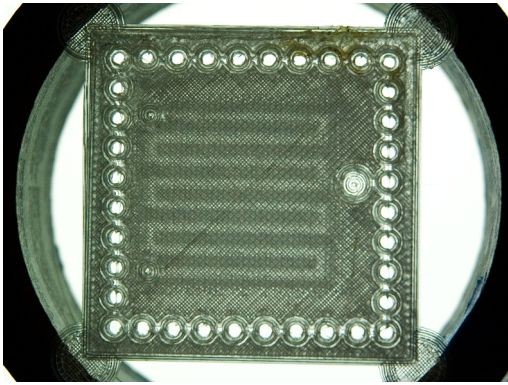
Fig. 7 Top view of the prototype. The architecture of the pipes are really clear, together with the three holes on the top layer.

IV. MEASUREMENT RESULTS

The first measurement that is carried out has the aim to verify the resonance frequency of the sensor when no liquid flows into the pipe. The measurements are demanded to a Anritsu 37347C VNA and the S_{11} parameter is collected from 2 to 5 GHz. Fig. 8 shows the measured resonant peak of the empty sensor at 4.06 GHz.

The following measurement is made by using distilled water to fill the pipe. A syringe is adopted to pump the fluid inside the cavity while the microfluidic sensor is under measurement. During this proces it is clear the frequency shift of the resonant peak toward lower frequency, monitored in real-time on the VNA screen. Once the tube inside the sensor is filled with water, the resonant frequency of the sensor is placed at 2.93 GHz (Fig. 8), with a shift of 5% with the respect of the simulated one.
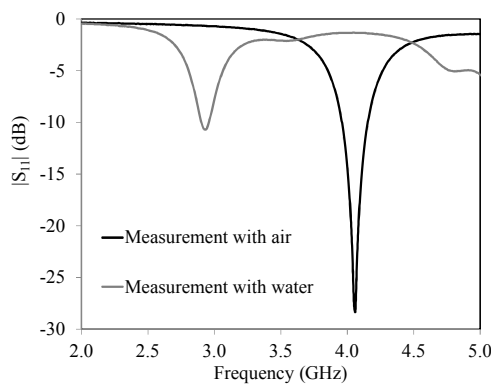

Fig. 8 Measured resonance peaks of the cavity when air or water fill the cavity. The frequency separation is up to 1.13 GHz.

This is a very important test because the very high dielectric permittivity of water. No liquids with higher dielectric constants are expected to be tested.

The graphs reported in Fig. 8 show how the resonance peak of the reflection parameter shifts because a variation in the dielectric constant. As expected the difference between the empty sensor and the water filled one is above 1 GHZ. In detail a total shift up to 1.13 GHz is measured. This is very important from the sensitivity point of view. This shift together with the good quality factor achieved results in a very high accuracy in testing differents fluids.

Measurements are promising for further tests with organic fluids and solutions, such as absolute ethanol. The dielectric permittivity of this alchol is close to 10 and the resulting resonance peak should be placed in the middle of the sensor frequency band (2.93-4.06 GHz). Because of the high sensitivity of the sensor, if the properties of two tested fluids are very close, their frequency separation will be high enough to be recognized and therefore estimate the different electromagnetic properties.

V. CONCLUSIONS

A novel techinque in design and fabrication of a microwave microfluidic sensor is proposed. The SIW technology is adopted to keep as high as possibile the quality factor of the structure with a consequent enhancing of the sensitivity of the device. The t-glase material is characterized and adopted for the 3D printing process. The first prototype is manufactured with high accuracy and the first measurements are promising for future testing with organic fluids.

REFERENCES

[1] E. MacDonald, R. Salas, D. Espalin, M. Perez, E. Aguilera, D. Muse, R.-B. Wicker, "3D Printing for the Rapid Prototyping of Structural Electronics," *IEEE Access*, Vol.2, pp. 234-242, Dec. 2014.

[2] C. Chua, K. Leong,and C. Lim, *Rapid Prototyping: Principles and Applications*, River Edge, NJ: World Scientific, 2003.

[3] S.-H. Yang, *Wireless Sensor Networks: Principles, Design and Applications*, Springer, 2014

[4] T. Chretiennot, D. Dubuc, K. Grenier, "A Microwave and Microfluidic Planar Resonator for Efficient and Accurate Complex Permittivity Characterization of Aqueous Solutions," *IEEE Transactions on Microwave Theory and Techniques*, Vol. 61, No.2, pp. 972-978, Feb. 2013.

[5] A.-A. Abduljabar, D.-J. Rowe, A. Porch, D.-A. Barrow, "Novel Microwave Microfluidic Sensor Using a Microstrip Split-Ring Resonator," *IEEE Transactions on Microwave Theory and Techniques*, Vol.62, No.3, pp. 679-688, March 2014.

[6] B.-S. Cook, J.-R. Cooper, M.-M. Tentzeris, "An Inkjet-Printed Microfluidic RFID-Enabled Platform for Wireless Lab-on-Chip Applications," *IEEE Transactions on Microwave Theory and Techniques*, Vol.61, No.12, pp. 4714-4723, Dec. 2013.

[7] R. Garg, I. Bahl, and M. Bozzi, *Microstrip Lines and Slotlines*, Third Edition, Artech House, May 2013.

[8] P.-I. Deffenbaugh, R.-C. Rumpf, K.-H. Church, "Broadband Microwave Frequency Characterization of 3-D Printed Materials," *IEEE Transactions on Components, Packaging and Manufacturing Technology*, Vol.3, No.12, pp. 2147-2155, Dec. 2013.

[9] Taulman3D website, http://taulman3d.com/t-glasefeatures.html, access Feb. 2015

[10] Printrbot website, http://printrbot.com/, access Feb. 2015

[11] F. Declercq, H. Rogier, "Permittivity and Loss Tangent Characterizatio for Garment Antennas Based on a New Matrix-Pencil Two-Line Method," *IEEE Transactions on Antennas and Propagation*, Vol. 56, No. 8, pp. 2548-2554, Aug. 2008.

[12] M. Bozzi, A. Georgiadis, and K. Wu, "Review of Substrate Integrated Waveguide (SIW) Circuits and Antennas," *IET Microwaves Antennas and Propagation*, Vol. 5, No. 8, pp. 909–920, June 2011.